Integrity Support Message Architecture Design for Advanced Receiver Autonomous Integrity Monitoring

Ilaria Martini, Markus Rippl and Michael Meurer
German Aerospace Center (DLR), Munich, Gemanny
email: Ilaria.Martini@dlr.de,
Markus.Rippl@dlr.de,
Michael.Meurer@dlr.de

***Abstract*—In the near future of multiconstellation and multifrequency GNSS signals, the users will experience a significantly increased accuracy, thanks to the larger number of satellites in view and to the ionosphere free observations. Integrity, continuity and availability requirements will mainly drive the system performance. In this scenario Advanced Receiver Autonomous Integrity Monitoring (ARAIM) has attracted significant interest, since it can provide aviation users with worldwide vertical guidance.**

This paper aims to contribute to the on-going discussion on the ARAIM design analyzing the critical problems and proposing recommendations for an Integrity Support Message (ISM) architecture satisfying the aviation integrity risk requirement and at the same time maximizing availability and continuity.

Several alternatives for different integrity risk allocation to the satellite, the GNSS ground, the ISM ground and the user are discussed. In particular three contributions are provided: an alternative approach for the overbounding method used to compute the integrity information, a ground monitoring algorithm for the estimation of the Integrity Support Message (ISM) and an ISM content design containing information in the satellite domain (along-track, cross-track and radial) rather than in the range domain. The improvement in terms of integrity, availability and continuity are shown by means of simulations results. In particular the reduction of conservatism of the proposed solution is presented.

BIOGRAPHIES

Ilaria Martini received the Master Degree in telecommunication engineering and the Ph.D. in information technology from the University of Florence, Italy. She was at the Galileo Project Office of ESA/ESTEC in 2003, working on the performance of the Galileo Integrity Processing Facility. She was research associate in 2004 at the University of Florence and in 2005 at the Institute of Geodesy and Navigation of the Federal Armed Forces Germany in Munich. In 2006 she joined the navigation project department of Ifen GmbH in Munich. Since 2012 she works as research associate in the Institute of Communication and Navigation at the German Aerospace Center (DLR), Oberpfaffenhofen. Her main area of interest is GNSS Integrity Monitoring.

Markus Rippl received his Diploma in Electrical Engineering and Information Technology from Technische Universitt Mnchen (TUM) in 2007. Since then, he has been a research fellow with the Institute of Communications and Navigation (IKN) at the German Aerospace Center (DLR), in Oberpfaffenhofen near Munich. His field of work is the integrity of GNSS-based navigation using receiver-side algorithms.

Michael Meurer received the diploma in electrical engineering and the Ph.D. degree from the University of Kaiserslautern, Germany. After graduation, he joined the Research Group for Radio Communications at the Technical University of Kaiserslautern, Germany, as a senior key researcher, where he was involved in various international and national projects in the field of communications and navigation both as project coordinator and as technical contributor. From 2003 till 2005, Dr. Meurer was active as a senior lecturer. Since 2005 he has been an Associate Professor (PD) at the same university. Additionally, since 2006 Dr. Meurer is with the German Aerospace Center (DLR), Institute of Communications and Navigation, where he is the director of the Department of Navigation and of the center of excellence for satellite navigation.

I. INTRODUCTION

The design of the Integrity Support Message (ISM) Architecture enabling the fulfilment of the aviation precision approach requirements for a standalone GNSS receiver with Advanced Receiver Autonomous Integrity Monitoring techniques is an interesting and challenging topic. This paper aims to contribute to the discussion providing guideline and recommendations for the optimum design. This introduction describes the context and identifies the problems addressed by the approach proposed in the second section.

First of all a short description of the background is provided. In particular the ICAO aviation integrity requirements, the ISM architecture design drivers and the present Advanced RAIM concept, are recalled. Secondly the problem of the error overbounding method, which imposes strict GNSS design requirements, is discussed. Finally the user point of view is analyzed with respect

to its need of relaxing requirements and simplifying the receiver algorithms.

A. Context

1) Integrity Requirements for aviation users

The objective of the ARAIM concept is to provide the aviation users with vertical guidance up to precision approach based on multiconstellation GNSS signals. Navigation systems supporting vertical guidance of aircrafts are subject to several requirements governing their performance. The requirements are standardized through the International Civil Aviation Organization (ICAO). The target operation levels are LPV, LPV-200 and beyond, which are specified in the ICAO Standards And Recommended Practices SARPs [1], as follows:

- fault-free accuracy 4m at 95% and 10m at 10^{-7},
- faulty-case accuracy 15m at 10^{-5},
- integrity risk $2 \cdot 10^{-7}$ per approach.

These represent the most strict requirements for GNSS applications at the present. They refer to small percentiles (10^{-7}) and to short operation intervals (approach duration of 150s), on which the user must be alerted within 6s when a failure condition occurs.

2) Advanced RAIM and ISM concept

The ARAIM concept was proposed within the U.S. GPS Evolutionary Architecture Study report [2]. Further evolution has been provided by the Working Group C ARAIM Technical Subgroup Interim Report [4]. The proposed receiver algorithm is based on the Multiple Hypothesis Solution Separation method described by [13].

To clarify the notation used in the rest of the paper, the ISM definition is briefly recalled (for details refer to [4] and [13])

The ISM contains two sets of parameters, one to describe overbounding distributions for integrity purpose and another to describe nominal performance for continuity purpose. The content in particular refers to the User Range Accuracy (URA) for GPS and to the Signal In Space Accuracy (SISA) for Galileo, both contained in the corresponding navigation message[1]. These values represent the standard deviations of the distribution overbounding the satellite orbit and clock errors, i.e. the Signal In Space Error (SISE). In particular the ISM for the i_{th} satellite contains:

- α^i: scaling factor for the $URA^i(SISA^i)$ to cover the integrity requirements,
- β^i: scaling factor for the $URA^i(SISA^i)$ to cover the continuity requirements,
- B^i_{max}: the maximum bias value of SISE to cover the integrity requirements,
- B^i_{nom}: the nominal bias value of SISE to cover the continuity requirements,
- P^i_{sat}: probability of single satellite fault.

Beside for each constellation, the ISM contains the term P_{const}, i.e. the probability of constellation wide fault.

3) ISM Architecture Design Drivers

The new concept of ISM/ARAIM represents an interesting possibility to meet the strict LPV integrity requirements. At present the architecture design is an open topic, containing several alternatives still to be screened.

Many aspects influence and determine the optimum design: liability constrains of the Aviation Navigation Service Providers (ANSP) and GNSS Providers, politic agreement among states and certification-standardization authorities, economic aspects related to the need to reuse as much as possible existing infrastructure, etc. This paper will focus only on the technical aspects. The aim is to contribute to the ongoing discussion, providing a methodology to address the main performance drivers and identifying guidelines and recommendations for the design.

The main ISM Architecture design drivers are the followings:

- the monitoring network in charge of collecting the observables used to compute the ISM content. Its coverage might be global (e.g. GNSS sensor stations network or even an Inter Satellite Link monitoring network), regional (e.g. SBAS like network) or local (e.g. GBAS like monitoring stations),
- the dissemination network in charge of sending the ISM to the final user. Its coverage might also be global (e.g. GNSS constellation or internet connection), regional (GNSS constellation transmitting regional information, or subset of a GNSS constellation, e.g. orbiting only on a specific region, GEO satellites) or local (VHF data link like VHF Data Brodcasting link of GBAS),
- the ISM latency, i.e. "the time it takes for the ground network to identify an issue in the space segment and alert the aircraft to that issue" [4].

Not all the combinations of the previous alternatives are feasible. Most of them do not provide the desired performance. The following sections analyze and identify technical constrains and guidelines for the optimization.

B. Relax GNSS architecture design requirements related to the error overbounding

One of the most critical issues of the GNSS integrity monitoring is estimating position error bounds covering small percentiles. The challenge is finding the best tradeoff between inflating the bound to be sufficiently safe and reach the required confidence level (i.e. 10^{-7}) without degrading excessively the continuity and availability. This problem is faced by the user and above all by the ground

[1] In case of GNSS system other than GPS and Galileo analogous values for $URA(SISA)$, characterizing the satellite orbit and clock errors, should be considered

segment when trying to provide integrity information to the user: either the GNSS ground monitoring in computing $URA(SISA)$ but also any other independent ground monitoring. A previous design of the Galileo integrity service showed in the past that the costs in terms of ground segment complexity are significant and should be carefully taken into account.

The idea at the present is that a third party can take part of the integrity risk. This could be the role of the independent ISM architecture. Through the provision of an additional integrity message, it could relax contemporaneously GNSS ground segment and user receiver requirements.

On the other side, it is important to have a clear and a common understanding of the most critical aspects, because the ISM architecture will need to address and solve the same problems of the GNSS ground monitoring. This section focuses in particular on the problems related to the overbounding method.

1) Overbounding concept

In many situations, the range error is difficult to be modeled a priori (i.e. in case of strong multipath, when only the non line of sight signal can be received and no a priori information can be used). But many stochastic errors are result of a combination of a large number of effects. For the central limit theorem the resultant statistic is Gaussian distributed. For this reason the overbounding is based on the Gaussian distribution model.

Another reason is that this distribution model simplifies the processing since the Gaussianity is conserved in linear transformations: if the ranging errors satisfy the overbounding in the range domain, the resultant position error will be Gaussian distributed with an overbounding standard deviation given by the covariance propagation method. This is guaranteed thanks to the linearity of the geometry transformation projecting the errors from the range to the user domain.

The overbounding concept allows deriving a conservative characterization of the position error from conservative models of the range error distributions.

Different definitions of Gaussian overbounding have been proposed in the past. ICAO defines the overbounding concept in [1] as follows:

If

$$\int_{y}^{+\infty} g_1(x)dx \leq \int_{y}^{+\infty} g_2(x)dx \quad \forall y \geq 0$$

and

$$\int_{-\infty}^{y} g_1(x)dx \leq \int_{-\infty}^{y} g_2(x)dx \quad \forall y \leq 0$$

$g_2(x) \sim N(0, \sigma)$ is a Gaussian distribution overbounding $g_1(x)$.

The ICAO concept, like the cumulative density function overbounding concept proposed by DeCleene in 2000 [6], is based on the assumption of zero-mean, symmetric, and unimodal distributions.

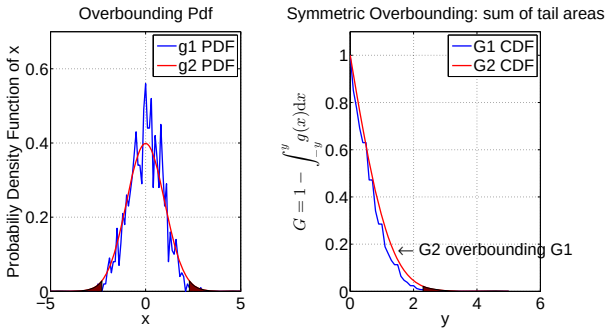

Figure 1: Symmetric overbounding concept. The sum of the left and right tails of the overbounding distribution exceeds that of the target distribution.

It might be interesting, as discussed for Galileo, trying to remove the symmetry assumption considering the sum of the tails, as shown in Figure 1, with the following definition:

If

$$\int_{-y}^{y} g_2(x)dx \leq \int_{-y}^{y} g_1(x)dx \quad \forall y \geq 0$$

$g_2(x) \sim N(0, \sigma)$ is a Gaussian distribution overbounding $g_1(x)$.

But in an equivalent way to [6], zero-mean and unimodality are required.

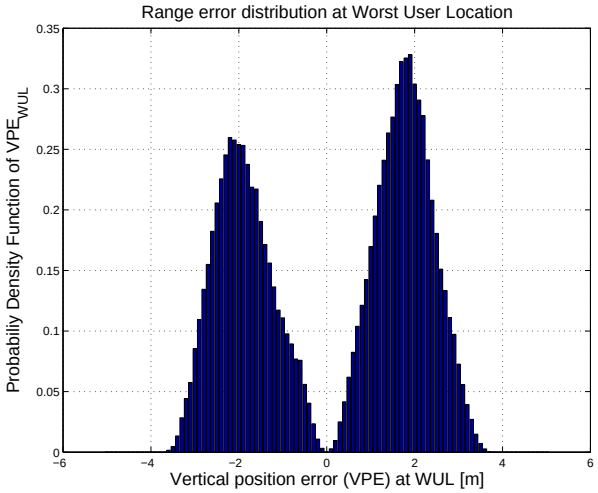

Figure 2: Statistic distribution of the vertical position error due to satellite orbit and clock at the worst user location, that is the maximum value of the signal in space error on the satellite visibility area.This distribution is generated in case of instantaneous SISE monitoring where each epoch the SISE for the worst user location is considered. The probability of SISE WUL being close to zero is also close to zero, in fact for any SISE vector its maximum projection in the range domain is always different from zero.

The zero-mean assumption represents a strong limitation, in fact, as the experience with WAAS suggests, small biases are always present and cannot be removed (e.g. antenna biases, signal distortions, etc.): the presence of biases must be then included in the range measurements model [2].

Besides also the unimodality and symmetry assumptions are restrictive: in fact the ground monitoring must conservatively protect the worst user location error, that is the maximum projection of the range error within the satellite footprint. This operation generates asymmetric and multimodal distributions like the one displayed in Figure 2, as described by [8].

Other concepts, proposed by [9], [10], [11], [12] overcome the mentioned limitations, because they allow asymmetry, multiple modes, and non-zero means. But these methods introduce a significant conservatism and generate large bound values which degrade continuity performance, as described in [15].

This is complicated by the fact that unfortunately the true error distributions are not known. The ground monitoring can only estimate them from a set of sample data. And the sample size is mostly significantly small to reach the 10^{-7} integrity risk confidence level.

For example a global network of 30 sensor stations needs at least 3 years to collect 10^8 samples at 1Hz from a constellation of 27 satellites. Instead considering an optimistic correlation time of 1 minute and a limited network coverage, more than 10 years are needed!

The lack of historic data is a problem not only for new GNSS systems, like Galileo, but also for existing systems, like GPS and WAAS, which are going to face a modernization period with new signals, new satellites and new error models (e.g. multipath error with dual frequency observations).

Furthermore the certification of the GNSS ground segment is characterized by stringent safety standards (DAL Level B). They impose even stricter requirements on the error bound estimation, which must be extremely accurate in particular during the verification phase.

In conclusion, the high confidence level required by the requirements, the lack of historic data and the conservatism of the overbounding methodologies are problems to be addressed for the definition of the ISM integrity concept, as it is described in the next.

2) Integrity Risk Allocation

This section describes the integrity risk allocation (for the notations refer to [1] and [14]) and presents in particular the role of the different systems involved: GNSS ground segment, ISM ground segment and user receiver algorithm (ARAIM). The scope is to analyze the impact of the overbounding risk on the integrity risk probability.

The overall integrity risk, that is the probability of having an Hazardous Misleading Information without an alarm being issued in time, is indicated with P_{HMI}. It has three main contributions: the fault free probability, P_{HMI}^{FF}, the narrow failure probability in case of failure affecting independently each satellite [2], P_{HMI}^{NF}, and the wide failure probability in case of simultaneous correlated satellite failures, P_{HMI}^{WF} [4].

[2]Independent failures can affect more satellites simultaneously.

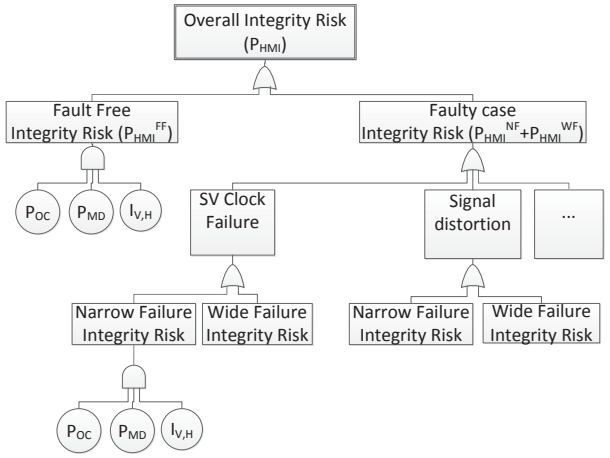

Figure 3: Integrity Risk Allocation Tree

Different threats are identified accordingly to the kind of failure they can generate (narrow or wide). Figure 3 shows an example of integrity risk tree, where only some threats are shown (satellite clock, satellite signal distortion, etc.). The threats (wide failures) that affect the whole constellation (i.e. earth rotation parameter failure [4]) are characterized by the constellation failure probability, P_{const}.

The overall integrity risk is given by the sum of the three contributions:

$$P_{HMI} = P_{HMI}^{FF} + P_{HMI}^{NF} + P_{HMI}^{WF}. \quad (1)$$

For the sake of simplicity in the next sections the focus of this analysis will be on the satellite failure probability, P_{sat}, i.e. on the P^{NF}. As described in [14], each integrity risk final node contains the product of the failure occurrence probability P_{OC}, the missed detection probability P_{MD} and the failure impact on the vertical and horizontal position error $I_{V,H}$:

$$P_{HMI} = P_{OC} P_{MD} I_{V,H} \quad (2)$$

The probability of occurrence P_{OC} depends on the number of failing satellites f and on the total number of satellites N. P_{OC} follows a binomial distribution:

$$P_{OC}(f, N) = \binom{N}{f} (1 - P_{sat})^{N-f} P_{sat}^{f} \quad (3)$$

Figure 4 shows that the occurrence probability of the multiple failure is smaller than twice the double failure one:

$$P_{OC}(f \geq 2, N) = \sum_{f=2}^{N} P_{OC}(f, N) \leq 2 P_{OC}(2, N) \quad (4)$$

Then the following upper bound for the integrity risk can be considered

$$P_{HMI} \leq P_{HMI}^{FF} + P_{HMI}^{NSF} + 2 P_{HMI}^{NDF} \quad (5)$$

with $P_{HMI}^{NDF} = P_{OC}(2, N)$.

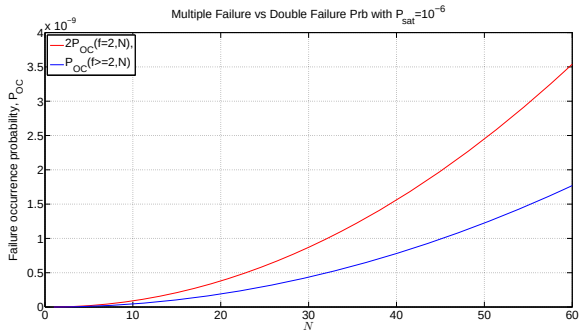

Figure 4: Comparison of occurrence probabilities between multiple satellite failure and double satellite failure case: $P_{OC}(f \geq 2, N) \geq 2P_{OC}(2, N)$. A $P_{sat} = 10^{-6}$ was used for the simulation. An analogous behavior is observed also for all $P_{sat} \in [10^-4, 10^-7]$.

Regarding P_{MD}, it is observed that in the fault free case no failure has to be detected, that is $P_{MD}^{FF} = 1$.

Besides for the failure cases the worst case is considered where no failure detection is performed at receiver level, i.e. $P_{MD}^{NSF} = P_{MD}^{NDF} = 1$ and all failure conditions generate HMI events on the user position, i.e. $I_{V,H} = 1$. This is a conservative approach, which has the scope to highlight and isolate the impact of the P_{sat} value on the integrity risk in the worst case.

It results

$$P_{HMI}^{FF} = (1 - P_{sat})^N I_{V,H} \tag{6}$$

$$P_{HMI}^{NSF} = N(1 - P_{sat})^{N-1} P_{sat} \tag{7}$$

$$P_{HMI}^{NDF} = \frac{N(N-1)}{2}(1 - P_{sat})^{N-2} P_{sat}^2 \tag{8}$$

Since $P_{sat} \ll 1$, Taylor series approximations for P_{HMI}^{NSF} and P_{HMI}^{NDF} can be used, obtaining

$$P_{HMI}^{NSF} \simeq NP_{sat} + o(P_{sat}^2) \tag{9}$$

$$P_{HMI}^{NDF} \simeq \frac{N(N-1)}{2} P_{sat}^2 + o(P_{sat}^3) \tag{10}$$

Finally, in the worst case conditions

$$P_{HMI} \leq (1-P_{sat})^N I_{V,H} + NP_{sat} + N(N-1)P_{sat}^2 + o(P_{sat}^2) \tag{11}$$

The resulting integrity risk allocation tree is shown in Figure 5.

The integrity risk in the narrow failure case is proportional to NP_{sat} and is the most critical one. In fact to have a P_{HMI} smaller than the 10^{-7} value specified by the integrity risk requirement, P_{sat} must be in the same order of magnitude.

Since P_{sat} is given by the contributions of the different threats, the design must identify for each threat with $P_{OC}I_{V,H} > 10^{-7}$ a barrier with a sufficiently small P_{MD}.

Whereas for most of the threats finding a barrier and tuning the relative P_{MD} might be not critical, the risk

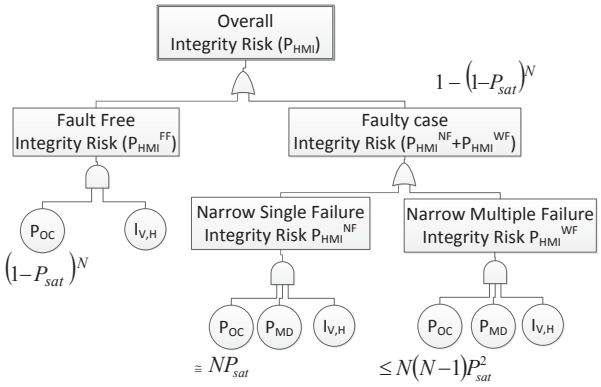

Figure 5: Satellite failure probability impact on the integrity Risk Allocation Tree. For the sake of simplicity the different threat contributions are not reported in the figure.

related to the overbounding remains problematic for all the intrinsic limitations described in the previous section.

This paper focuses on reducing the impact of this risk through the ISM independent architecture, allowing an effective relaxation of the GNSS ground monitoring design requirements.

C. Relax receiver design requirements related to Time To Alarm performance

The integrity risk requirements are expressed in terms of tail probability area. The user actually needs that each instantaneous position error does not generate an HMI event. Unfortunately the stochastic processes are not stationary and any outlier must be monitored.

The detection of high dynamic error has been up to now allocated to RAIM Fault Detection and Exclusion techniques. For precision approach operations, their performances need to meet TTA and continuity requirements on short operation durations (150s). If ISM could monitor also high dynamic error, the user requirement could be significantly relaxed, reducing in particular the receiver algorithm complexity.

More in details, the ISM design is based on the following parameters:

- TIA (Time to ISM Alarm): interval between the ISM reception time at the user receiver and the time of failure occurrence,
- T_{obs}: duration of the interval on which the ISM ground segment collects observations to compute the ISM content,
- T_{diss}: duration of the interval between the ISM transmission time and the ISM reception time at the user receiver. The ISM computation duration is included in this term and can be considered negligible.
- UR_{ISM}: update rate of the ISM content

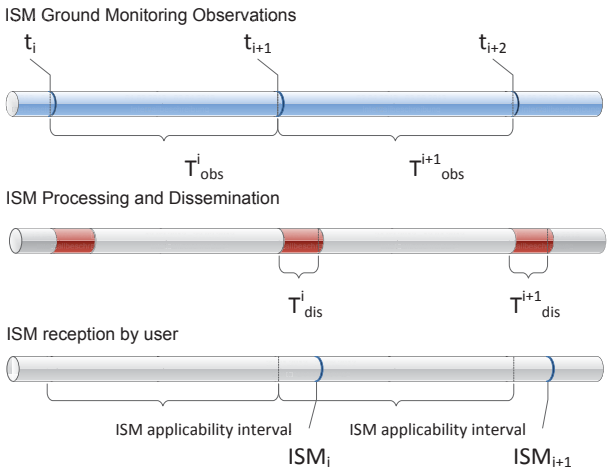

Figure 6: Relationship between TIA, T_{obs} and T_{diss}

Figure 6 shows the relationship between TIA, T_{obs} and T_{diss}.

It is observed that $TIA_{max} = T_{obs} + T_{diss}$. Besides if no overlapping observation intervals are considered, as shown in the figure, $UR_{ISM} = \frac{1}{T_{obs}}$. Actually, as it is discussed in the next, to monitor almost stationary process and slow changing errors it is suggested to consider overlapping intervals (long term monitoring).

Depending on the value of UR_{ISM}, two types of monitoring can be identified as extreme cases. Then the final ISM could be any solution in between as well as a combination of both.

1) Long term monitoring

If ISM aims to monitor only the fault free nominal conditions (overbounding) or slow dynamic error for the faulty case, the ISM does not need to have a high update rate. In this case the ISM content must be a prediction of the error bound on the future before the next ISM is received. This means that the ISM ground monitoring can only monitor almost stationary processes and/or detect small drifting errors, which might generate in the next interval an HMI event for the user.

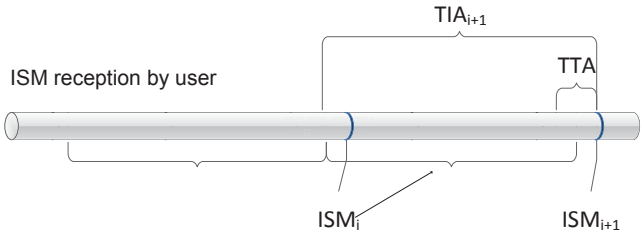

Figure 7: Long term monitoring: relationship between TIA versus TTA. In this case the ISM refers to the future

Figure 7 shows the meaning of the ISM, that is a prediction on the future interval and its relationship with TTA.

2) Short term monitoring

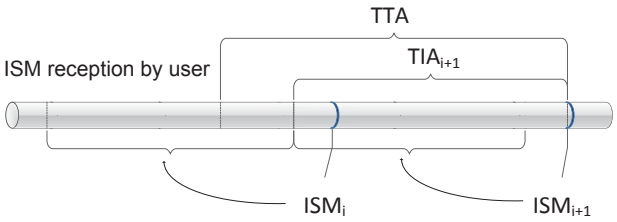

Figure 8: Short term monitoring: relationship between TIA versus TTA. In this case the ISM refers to the past (if $TIA < TTA$)

If ISM aims to address high dynamic failures, it could be interpreted as a bound on the past 6s, as displayed in Figure 8.

The ISM design requirements are in this case

- $TIA < TTA$,
- $T_{diss} \ll TTA$,
- $UR_{ISM} > 1/TTA$.

In this hypothetic extreme case the ISM must be updated at least every 6s and above all the dissemination delay must be significantly smaller than the TTA. This second approach has the advantage to protect the user against large instantaneous failure, which must be otherwise detected by the user. This approach relaxes and simplify the user integrity monitoring at receiver level.

On the other side the ARAIM concept is based on the independence of the integrity service from the ground monitoring. The possibility to provide a shorter term monitoring introduced in this paper refers to a short latency however bigger than the 6s, e.g. in the order of minutes. A Fault detection and exclusion algorithm must be used in any case by the user, because ISM would cover only the satellite and constellation failures. But the missed detection requirements for the receiver algorithm would be relaxed.

II. ISM Ground Monitoring Algorithms

This section contains the description of the ISM data content and the ISM ground monitoring algorithm able to overcome the problems described in the previous section.

The ISM computation algorithm is divided in two parts.

The first one is a long term monitoring aiming to cover the fault free integrity risk. It assesses the validity of the GNSS nominal performances represented by the $URA(SISA)$ values. In case these values do not perform a correct overbounding, inflation factors are estimated and sent to the user through the ISM. This part impacts on the ISM architecture design in particular on the monitoring

network. In fact its coverage must enable to reach the required confidence level by collecting a sufficient amount of data.

The second part is a short term monitoring aiming to cover the faulty case integrity risk. This part strongly depends on the ISM update rate and consequently impacts on the ISM architecture, i.e. on the dissemination network coverage.

A. ISM content and format

The bandwidth available to transmit the integrity information might be limited, as in the case of the $URA(SISA)$ information sent through the GNSS navigation message. Although the satellite orbit and clock error (SISE) can be estimated by the GNSS ground segment as vector of three components (along-track, cross-track and radial [8]), the integrity information sent to the user through the navigation message, $URA(SISA)$, contains scalar values bounding the errors in the range domain.

The bounding in the range domain is more conservative than that in the satellite domain. In fact, since any user in the satellite visibility area has to be protected, the integrity bounds are inflated to protect an hypothetic user in the worst location. This might degrade significantly the continuity and availability, as it shown in the result section.

This paper suggests to send the vectors of values bounding the errors in the satellite domain (along-track, cross-track and radial) rather than the scalar ones in the range domain. The projection in the range domain is then performed by the user itself. This approach better fits with the real user performance. Beside all the involved algorithm transformations are linear and the Gaussian statistic properties are conserved after the convolution: the multimodal distribution effect, shown in Figure 2, is not present anymore. The achievable improvements are shown in the result section.

The integrity concept proposed in this paper defines the following ISM data content for the i_{th} satellite:

- $\underline{\alpha}^i$: vector of scaling factors for the standard deviation of the along-track, cross-track and radial satellite orbit and clock error components,
- $\underline{B}^i_{nom}$: vector of mean values of the along-track, cross-track and radial satellite orbit and clock error components,
- $\underline{B}^i_{max}$: vector of maximum values of along-track, cross-track and radial satellite orbit and clock error components.
- P^i_{sat}: probability of single satellite fault

For the whole constellation, P_{const}, i.e. the probability of constellation wide fault is contained in the ISM.

Table 1 compares the ISM parameters baseline ([4]) and the one proposed in this paper. The proposed ISM content differs from the [4] for the following aspects:

Table 1: ISM content baseline versus the proposed one

ISM baseline	**ISM proposal**
α^i: scaling factor for the $URA^i/SISA^i$ to cover the integrity requirements	$\underline{\alpha}^i$: vector of scaling factors for the standard deviation of the along-track, cross-track and radial satellite orbit and clock error components
β^i: scaling factor for the $URA^i/SISA^i$ to cover the continuity requirements	-
-	$\underline{B}^i_{max}$: vector of maximum values of along-track, cross-track and radial satellite orbit and clock error components
B^i_{nom}: the nominal bias value of SISE to cover the integrity requirements	$\underline{B}^i_{nom}$: vector of mean values of the along-track, cross-track and radial satellite orbit and clock error components
P^i_{sat}: probability of single satellite fault	P^i_{sat}: probability of single satellite fault
P_{const}: probability of constellation fault	P_{const}: Probability of constellation wide fault

- the information are vectors of three components instead of scalars (except the satellite and constellation failure probability, which are scalars in both cases),
- the term β^i is not included in the proposed ISM. In case the ARAIM MHSS algorithm uses a distinction between continuity and integrity parameters [4], a constant factor between α^i and β^i can be used, as proposed in the GEAS report [2]: $\beta^i = 0.5\alpha^i$,
- the $\underline{B}^i_{max}$ term contains information on the error upper bound instead of the error distribution mean value. This allows a more effective failure detection and integrity risk reduction, as explained hereinafter,
- the $\underline{B}^i_{nom}$ term contains the mean values of the SISE components, whose confidence level addresses the integrity performance and not the continuity ones.

Table 2: ISM latency

Parameter	Monitoring type	Latency
$\underline{\alpha}^i$	long	weeks
$\underline{B}^i_{nom}$	long	weeks
P_{sat}	long	months
P_{const}	long	months
$\underline{B}^i_{max}$	short	seconds or minutes

Table 3: ISM maximum data rate at 0.2 Hz

Parameter	Number of bits	Data rate in bps
$\underline{\alpha}^i$	5760	1152
$\underline{B}^i_{nom}$	5760	1152
$\underline{B}^i_{max}$	5760	1152
P_{sat}	1920	384
P_{const}	64	13
Total ISM	25024	5005

The ISM is constituted of two parts: the $\underline{\alpha}^i$, $\underline{B}^i_{nom}$, P^i_{sat} and P_{const} estimated by the long term monitoring,

which can and should have a long latency and the $\underline{B}^i_{max}$ estimated by the short term monitoring, which should have a short latency, as shown in Table 2. This short latency content must not necessarily be updated every 6s. The proposed approach can be applied also with a smaller update rate. Each region and ASNP can decide independently and provide different services to the user.

The intent is to provide the user also with a shorter latency monitoring, which enables on one side the estimation of slow dynamic threats and on the other the estimation of the real satellite and constellation performance. In fact the integrity model of $URA(SISA)$ is too conservative and more realistic parameters, like URE or those provided by a short term monitoring, are needed by the user.

Table 3 shows an estimation of the maximum ISM data rate reached if hypothetically an ISM latency smaller than 6s is used to transmit all the parameters (update rate 0.2 Hz)[3]. This estimation is provided to assess in a worst case of a single dissemination link the maximum bandwidth needed. The maximum data rate would be circa 5 Kbps, which can fit in a local dissemination link like the GBAS VHF Data Link (maximum datarate is 31 Kbits/s [3]). In case of a global dissemination a satellite link can sustain such a bit rate.

B. Long term integrity monitoring

The long term monitoring must

- verify whether the $URA(SISA)$ navigation message information perform the overbounding and if necessary to compute the relative inflation factors $\underline{\alpha}^i$,
- assess the nominal bias of the signal in space error, $\underline{B}^i_{nom}$,
- eventually, estimate and adjust the P_{sat} and P_{const} values specified by the GNSS providers.

Regarding the first point, the estimation of the standard deviation, σ, overbounding a certain distribution, is usually performed estimating the sample standard deviation and taking the upper limit of the corresponding confidence level. In particular an unbiased estimator, used when the sample size is very large, is the standard deviation of the sample, denoted by S_N and defined as follows:

$$S_N = \sqrt{\frac{1}{N-1}\sum_{i=1}^{N}(x_i - \overline{x})^2}$$

where $\{x_1, x_2, ..., x_N\}$ are the observed values of the sample items and $\overline{x}$ is the sample mean value of these observations, while the denominator N stands for the sample size.

[3]A constellation of 30 satellites and 1 double for each parameter were assumed

Since $\frac{(N-1)S_N^2}{\sigma^2}$ follows a chi square distribution with $N-1$ degrees of freedom, the following can be stated

$$P\left(\frac{(N-1)S_N^2}{\sigma^2} \leq \chi^2_{N-1,1-CL}\right) = 1 - CL$$

where CL is the confidence level. Equivalently

$$P\left(S\sqrt{\frac{N-1}{\chi^2_{N-1,1-CL}}} \leq \sigma\right) = 1 - CL$$

The value $\sqrt{\frac{N-1}{\chi^2_{N-1,1-CL}}}$ is taken as inflation factor $\underline{\alpha}^i$ for the standard deviation of the distribution overbounding the true one.

This paper proposes another method, called quantile method and described hereafter. The improvement in terms of reduced inflation factors is presented in the result section.

1) Overbounding risk as threat

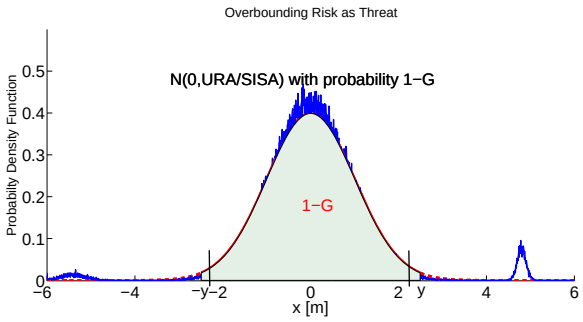

Figure 9: The sample size N used to assess a certain empirical distribution identifies a maximum interval $[-y, y]$ for which the overbounding can be estimated. Only the following assertion can be done: $P(|x_i| < y) = 1 - G$. Outside the interval, the lack of information and the degraded test accuracy don't allow to perform any assessment.

As described in the first section, the ground monitoring, both the GNSS than the ISM one, has a limited sample size available to assess the small percentiles of the nominal distribution. Overbounding can be estimated only for a certain maximum percentile, depending on the sample size N. If the maximum percentile which can be assessed with enough accuracy is indicated with G, it can be argued only that with probability $1 - G$, the sample x_i belongs to the central area of the Gaussian distribution characterized by the $URA(SISA)$. As shown in Figure 9, only the following assertion can be done:

$$P(|x_i| < y) = 1 - G$$

On the tails of smaller percentiles, no assertion can be done, since not enough information is available.

This has an impact on the satellite failure probability, P_{sat}. In fact this value is the result of all possible failure probabilities. It is based on design requirements, assessed by the GNSS provider and verified by the ISM system provider. The overbounding risk, that is the risk

that the x_i belongs to the tails, should be defined as threat and be included in the P_{sat} probability, as follows

$$P_{sat} = \sum_{j=0}^{N_{threats}} P_{threat}^{j} + G$$

This approach allows avoiding the use of overbounding methodologies which introduce conservative inflation factors, degrading significantly the continuity and availability performance and based in any case on unverifiable assumptions. And at the same time, it can significantly relax the ground segment requirements, which does not need anymore to guarantee bounding till small percentiles.

2) Quantile Methodology

The methodology proposed to assess this long term statistic is based on an hypothesis testing approach using quantile estimation. The algorithm takes also into account the estimation accuracy related to the limited sample size.

The objective is to assess whether the $URA(SISA)$ value performs the overbounding of the $SISE$ distribution. This is done observing the empirical distribution of the $SISE$ estimations.

The following notation is used: $SISE$ is the scalar value containing the satellite orbit and clock error in the range domain and $\underline{SISE}$ is the vector containing the same error in the satellite domain (i.e. long-track, across-track and radial components)[4].

The computation of the empirical distribution is based on the samples collected on a certain long batch. The overbounding of the $URA(SISA)$ is assessed with an hypothesis testing methodology estimating the quantiles. This method allows to take a margin to control the risk of erroneous failure of the assessment (the ground monitoring assessment is wrong due to statistical uncertainty although overbounding in terms of probability indeed was given). This is important above all when sample distribution are generated with small sample size.

The samples are generated by the ground monitoring by assessing the satellite orbit and clock failure error vector, $\underline{SISE}$. In particular several GSS observations are collected by in the ground segment, pre-processed, corrected for the network synchronization error, and finally a least square estimation based on the GNSS residuals is performed [8]. The algorithm considers separately the three components of the estimated $SISE$ and for each of them verifies the overbounding.

$URA(SISA)$ performs the overbounding of the true distribution for any boundary y if the following conditions are satisfied [5]

$$G_l(y) \leq \overline{G_l}(y) \forall y \geq 0 \tag{12}$$

and

$$G_r(y) \leq \overline{G_r}(y) \forall y \geq 0 \tag{13}$$

where the left and right tail weights of the real distribution with probability density function $g(x)$ are

$$G_l(y) = \int_{-\infty}^{-y} g(x)dx \tag{14}$$

$$G_r(y) = \int_{y}^{\infty} g(x)dx \tag{15}$$

and the left and right tail weight of the nominal distribution with probability density function $\overline{g}(x)$ are

$$\overline{G}_l(y) = \int_{-\infty}^{-y} \overline{g}(x)dx \tag{16}$$

$$\overline{G}_r(y) = \int_{y}^{\infty} \overline{g}(x)dx \tag{17}$$

with $\overline{g} = N(0,$URA(SISA)$)$.

The probabilities G_l and G_r cannot be exactly determined. They can be estimated by determining the frequency of samples that are respectively less than y and greater than +y:

$$\hat{G}_l(y) = \frac{n_{l,y}}{N} \tag{18}$$

and

$$\hat{G}_r(y) = \frac{n_{r,y}}{N} \tag{19}$$

where $n_{l,y}$ is the number of samples x_j with $x_j < -y$, $n_{r,y}$ is the number of samples x_j with $x_j > y$ and N total number of samples. To simplify the algorithm, the $SISE$ samples x_j are normalized with respect the $URA(SISA)$ values to be verified. With this normalization the tail areas can be compared directly with standard normal tails.

This estimation is repeated for different y values and performed separately for each error component[6].

The method considers separately the verification of the left and right tail and then combine the inflation factors taking the maximum of both. Hereafter the algorithm for the left tail, for one percentile and one error component is explained.

An hypothesis test method is used, defining the following hypothesis:

$$\begin{aligned} H_0 &: G_l(y) \leq \overline{G}_l(y) \\ H_1 &: G_l(y) > \overline{G}_l(y) \end{aligned} \tag{20}$$

The important assumption is taken that the observed samples are mutually uncorrelated. The correlation time is assumed known "a priori", provided by the GNSS system provider or estimated during a preliminary ground

[4]The satellite clock is modeled in the radial component in order to reduce the number of unknowns and take advantage of the redundancy.

[5]The ICAO overbounding definition is considered as reference [1]

[6]Since $URA(SISA)$ refers to the norm of the $\underline{SISE}$ vector, a scaling factor $(1/\sqrt{3})$ should be included in the normalization. But the $URA(SISA)$ values bound the vector projection and not the vector norm. Then for safety reason the scaling factor is not included. Nevertheless for algorithm tuning, this aspect should be taken into account and eventually the scaling factor included.

monitoring initialization phase. The correlation time must be taken into account for the sampling rate.

The number of tail samples $n_{l,y}$ follows a binomial distribution:

$$P(n_{l,y} = x) = \binom{N}{x}(1-p)^{N-x}p^x, \tag{21}$$

where $p = G_l(y)$.

In order to guarantee a certain α-risk, that is the probability of erroneously rejecting the H_0 hypothesis, the threshold x_T for this binomial distribution is computed for which

$$P(n_{l,y} > x_T) \leq \alpha \tag{22}$$

where

$$P(n_{l,y} > x_T) = 1 - \sum_{n=0}^{x_T}\binom{N}{n}(1-\overline{p})^{N-n}\overline{p}^n \tag{23}$$

and $\overline{p} = \overline{G}_l(y)$.

The corresponding threshold for the sample frequency is given by

$$p_{l,T}(y) = x_T/N \tag{24}$$

It is observed that with this test threshold, for any value of G_l for which $G_l(y) < \overline{G}_l(y)$, the probability of erroneously rejecting H_0 is smaller than the α-risk, as shown in Figure 10.

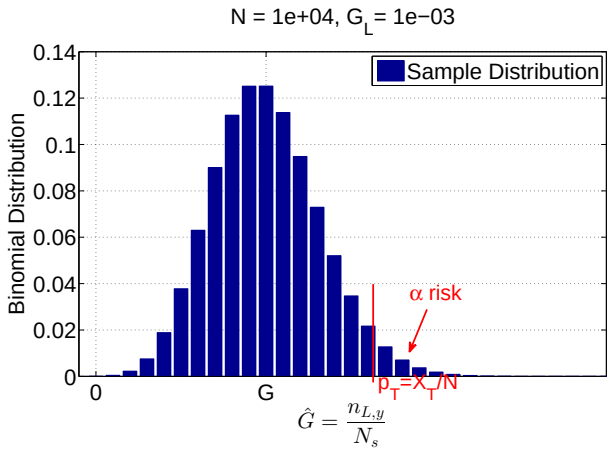

Figure 10: Hypothesis Testing Threshold

The overbounding is verified, if for each considered boundary y the observed frequency of samples bigger than y is less or equal to the corresponding threshold.

$$\hat{G}_l(y) \leq p_T(y) \tag{25}$$

In case the overbounding test is not passed, an inflation factor $K_l(y)$ is computed. In particular for each y, the minimum inflation factor $K_l(y)$ is found, for which the number of samples $n^K_{l,y}$, for which $\frac{x_i}{K_l(y)} \leq y$ satisfies

$$\hat{G}^K_l(y) = \frac{n^K_{l,y}}{N} = p_T(y) \tag{26}$$

Afterwards the maximum is taken among different y

$$K_l = \max_y K_l(y) \tag{27}$$

and between the left and right tail inflation factors:

$$K = \max(K_l, K_r) \tag{28}$$

Table 4: Hypothesis Test Thresholds and minimum detectable tail with $N = 1000$, $\alpha = 10^{-3}$ and $\beta = 10^{-2}$

y	Standard Tail $G(y)$	Left/Right Tail Threshold $p_T(y)$	Minimum Detectable Tail $G_{MD}(y)$
0.5	0.3085	0.3540	0.3902
1.0	0.1586	0.1950	0.2258
1.5	0.0668	0.0920	0.1154
2.0	0.0227	0.0390	0.0556
2.5	0.0062	0.0150	0.0265
3.0	0.0013	0.0060	0.0145
3.5	0.0002	0.0030	0.0100

The overbounding test thresholds, given a certain α-risk, are computed offline and a lookup table is used to perform the test. An example is provided in Table 4.

The algorithm is performed and repeated separately for each satellite and error component and provides the values of $\underline{\alpha}^i$, that is the estimated K factors.

It is possible to characterize the test accuracy observing the algorithm resolution shown in Table 4. In fact given a certain hypothesis test threshold, a β-risk can be defined and the relative minimum detectable tail area identified. G_{MD} is the minimum value of $G > \overline{G}$ for which the probability of erroneously deciding for H_0 is smaller than β-risk.

The difference

$$\frac{G_{MD} - \overline{G}}{\overline{G}}$$

represents the relative test resolution and provides a measurement of the algorithm accuracy for which the missed detection capability is guaranteed.

3) Algorithm

The long term ISM ground monitoring aims checking whether $URA(SISA)$ performs the overbounding and if not, it computes inflation factors for $URA(SISA)$ and send them to the user through the ISM. The algorithm outputs are the $\underline{\alpha}^i$ vector for each satellite, given as input the samples of the estimated $\underline{SISE}$ components and the $URA(SISA)$ navigation message information. The algorithm steps, for satellite i and each error component, $SISE_j$ of the $\underline{SISE}$ vector, are the following:

1) For each y value in the Table 4,
   a) Compute the N samples

$$x_t = \frac{SISE_{j,t}}{\sigma}$$

with $\sigma = URA$ for GPS, $\sigma = SISA$ for Galileo satellite and $t = 1...N$,

b) Compute the relative frequency

$$\hat{G}_l(y) = \frac{n_l}{N}$$

where n_l is the number of samples x_t for which $x_t < -y$,

c) Compare the relative frequency $\hat{G}_l(y)$ with $p_{l,T}$ corresponding to current y contained in Table 4,

d) If $\hat{G}_l(y) > p_{l,T}$, find iteratively the minimum $K_l(y)$ value for which

$$\hat{G}_l^K(y) = \frac{n_l^K}{N} \leq p_{l,T}$$

where n_l^K is the number of samples x_t for which $\frac{x_t}{K_l(y)} < -y$,

e) If $\hat{G}_l(y) \leq p_{l,T}$, set $K_l(y) = 1$,

2) Compute the $K_l = \max_y K_l(y)$,

3) Compute the inflation factor K_r for the right distribution tail analogously to the left tail one, K_l,

4) Compute $\alpha_{i,j} = \max(K_l, K_r)$.

Besides, the mean value of each $\underline{SISE}$ component and for each satellite is assessed as follows

$$B_{nom,j} = \frac{1}{N}\left|\sum_{j=0}^{N} SISE_j\right| + \frac{t_{c,N-1}\sigma}{\sqrt{N}}$$

where $\sigma = \alpha_{i,j} URA$ for GPS and $\sigma = \alpha_{i,j} SISA$ for Galileo and $t_{c,N-1}$ is the percentile value of a t-Student distribution with $N-1$ degrees of freedom relative to the confidence level c. The confidence level is derived by the maximum y value verifiable with the available sample size, N.

Finally the P_{sat} and P_{const} can be verified. In particular these probabilities can be assessed evaluating the relative frequency of respectively the satellite and constellation failures on the whole available data history. These estimations are compared with the values specified by the GNSS providers and/or eventually conservatively updated through the ISM.

It is in any case suggested to use for P_{sat} and P_{const}, the values specified by the GNSS providers. Their estimation at ISM should be discarded due to the no stationarity of the processes involved and to the long observation period required to reach a significant confident estimation.

C. Short term integrity monitoring

The possibility to introduce also a short term monitoring has the scope to characterize more closely the constellation and satellite performance and cover part of the integrity risk for the faulty case. This is performed by computing the error parameters, $\underline{B}^i_{max}$, which contain upper bounds of the signal in space errors.

[2] and [4] indicate that the $\underline{B}^i_{max}$ values represent a conservative estimation (maximum) of the mean values of the SISE distribution.

This paper proposes to use this term in order to cover high dynamic failures and relax the receiver FDE requirements. To cover the failure condition, the $\underline{B}^i_{max}$ value should provide information on the tail area, more than on the mean value [5]. This is done by fixing a priori a certain risk probability γ and observing each satellite error component, $SISE_j$, on a certain interval. The $SISE_j$ upper limit, $B_{max,j}$, is then computed, in order to have

$$P(\left|SISE^i_j\right| \geq B^i_{max,j}) \leq \gamma$$

To relax the user requirements for the instantaneous failure detection, the short term monitoring should ideally be updated at least every 6s (TTA). In this way the ISM ground monitoring could compute the maximum value of the $SISE$ on intervals of 6s. This value is then inflated to take into account the ground estimation accuracy provided by the inverse diluition of precision and the sensor stations range noise. The obtained value would represent the $\underline{B}^i_{max}$ value. But this approach would represent a SBAS-like integrity service. And for ARAIM it is intended to have an ISM latency bigger than the TTA.

With $TIA > TTA$ (or $TIA \gg TTA$), the ISM ground monitoring can still detect slow dynamic errors, i.e. small drifting errors. For a given short term TIA, the specific error dynamic detectable by the ISM short term monitoring must be identified. The ISM short term monitoring can address only the identified errors characterized by the a priori model. To this purpose, it can estimate the error drift corresponding to the model, predict the error on the future interval and detect possible HMI event. The $\underline{B}^i_{max}$ is then a prediction with confidence level γ of the maximum error during the next operation interval. This covers only the errors with the dynamic identified a priori. It does not exclude the occurrence of big outliers generated by higher dynamic errors.

In this case the integrity risk allocation must distinguish between slow dynamic and high dynamic threats and identify separately the detection strategy. With $TIA > TTA$, part of the detection of high dynamic failures must be allocated to the user ARAIM algorithm.

The short term monitoring should be in charge also to flag a satellite as unhealthy (by setting for example the $\underline{B}^i_{max}$ parameters to invalid value, e.g. -1) in case of large and persistent errors. The user can then discard the satellites declared unhealthy by the ISM ground monitoring.

Since $\underline{B}^i_{max}$ contains the three vector components, the unhealthy flag should be set independently for each of them, allowing a selection strategy at receiver level, depending on the specific geometry and requirement. For example a user interested only on lateral guidance (e.g. a ship or an aircraft not in a final approach phase, etc.) might in any case want to use satellites at zenith with radial $SISE$ component flagged as unhealthy.

D. User algorithm

The user algorithm which mostly suits the short latency approach is similar to the integrity risk algorithms,

proposed by Oehler [7] and that proposed by Mach [5] for Galileo. The most important advantage of this concept is that the integrity risk allocation is not fixed among vertical and horizontal components, as in [4]. The user does not compute a protection level, but calculates directly the integrity risk at alert limit level ([7]).

But the proposed algorithm has the following important differences:

- for the fault free mode the signal in space error distribution to be considered is not a zero mean Gaussian distribution with standard deviation $URA(SISA)$, $N(0, URA(SISA))$, but three biased Gaussian distributions for the along-track, cross-track and radial signal in space error with inflated standard deviations $N(B^i_{nom,j}, \alpha^i_j \cdot URA(SISA))$,
- for the faulty mode the signal in space error must be considered bounded by $B^i_{max,j}$ with a risk probability γ ([5]),
- multiple failures are included in case the occurrence failure probability is not negligible with respect to the integrity risk.

The user estimates the overall integrity risk by adding several contributions, from fault free to single and multiple failure cases. Each contribution is given by the tail area delimited by the alert limit. Each faulty case should be included only if the relative probability of occurrence P_{OC} is not negligible with respect to the integrity risk.

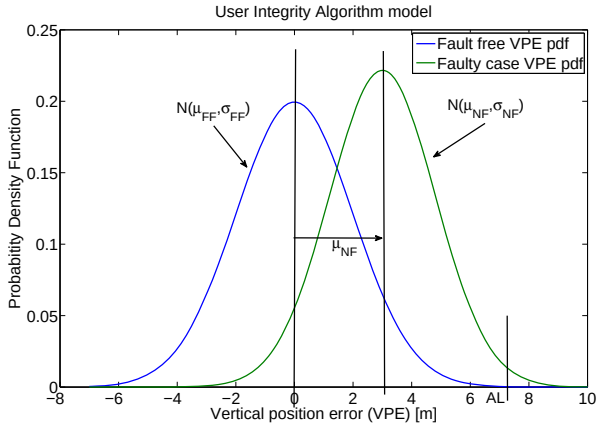

Figure 11: User integrity algorithm: vertical position error distributions for the integrity risk user algorithm.

Figure 11 shows the vertical position error distributions considered for the integrity risk computation. In the plot only the fault free case and the narrow single faulty case are displayed. The user algorithm considers also, if needed, the multiple failure case.

Before starting with the integrity risk computation, the user has to project the signal in space vectorial information ($\underline{\alpha}$, $\underline{B_{nom}}$ and $\underline{B_{max}}$) into the range domain (α, B_{nom} and B_{max}).

The vertical position error distribution is a Gaussian distribution, whose mean value μ_{FF} and the standard deviation σ_{FF} are obtained considering for all range errors the fault free Gaussian distribution $N(B_{nom}, \sqrt{\alpha\sigma^2_{sv} + \sigma^2_{tropo} + \sigma^2_{user}})$, with $\sigma_{sv} = URA$ for GPS and $\sigma_{sv} = SISA$ for Galileo. Estimation models of the tropospheric and receiver local error, i.e. σ_{tropo} and σ_{user}, are provided in [4].

The faulty case mean value μ_{NF} and the standard deviation σ_{NF} are obtained considering for all fault-free range errors the Gaussian distribution $N(B_{nom}, \sqrt{\alpha\sigma^2_{sv} + \sigma^2_{tropo} + \sigma^2_{user}})$ and for the faulty range error the distribution $N(B_{max}, \sqrt{\sigma^2_{tropo} + \sigma^2_{user}})$. In fact the satellite orbit and clock error contributions are already contained in the inflation of $B_{max,j}$ and its corresponding risk probability γ.

The fault and detection exclusion algorithm based on the solution separation method proposed by the MHSS algorithm [4] must be used in both cases to have the necessary failure detection capability at receiver level.

III. Results

This section presents the performance of the proposed integrity concept and the ISM processing algorithms by means of Monte Carlo simulations.

A. ISM content in the satellite domain

If ISM contains vectors bounding the single error components instead of scalars, integrity, continuity and availability performance are improved. This section shows the improvement in term of reduction of the ISM parameters.

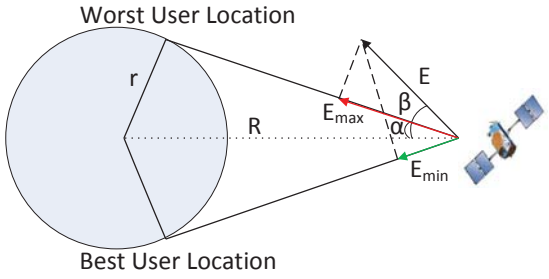

Figure 12: Signal In Spacer Error vector projected within the satellite footprint. The worst user location (WUL) and the best one (BUL) are identified. In the figure $r = 6371km$, $R = 26600km$ and $\alpha = 13.86$. The user masking angle is assumed zero.

Different Signal In Space Errors, E in Figure 12, have been generated and their projections in the satellite visibility area have been analyzed. In particular the ratio between the minimum and the maximum projections has been observed. The goal is estimating the degradation experienced by a user located in the best user position when applying the error of the worst user location. Figure 12 shows the geometry of the problem.

Figure 13 shows the ratio between the minimum and the maximum projection for different angles β,

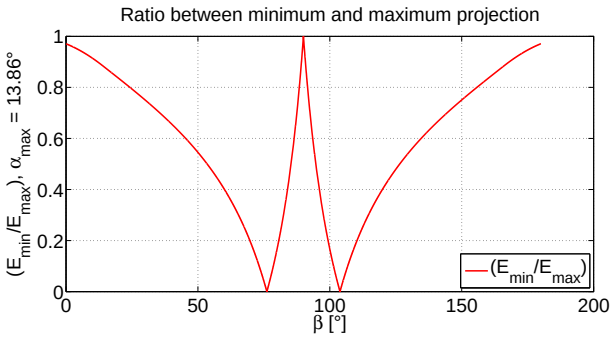

Figure 13: Ratio between the maximum and the minimum SISE projection in the satellite visibility area versus the angle β.

$$R(\beta) = \left| \frac{E_{min}}{E_{max}} \right|$$

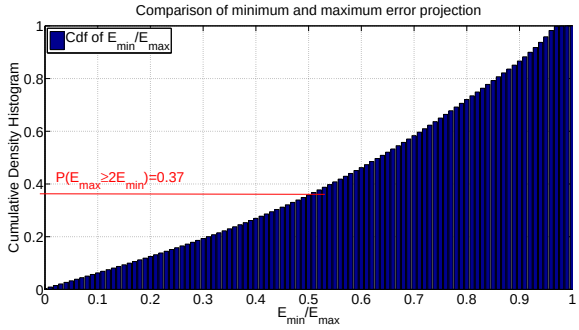

Figure 14: Cumulative distribution of the ratio $R(\beta) = \left| \frac{E_{min}}{E_{max}} \right|$

and Figure 14 the relative cumulative density histogram. Both plots show that there are many cases, where a user located in the best position can experience an inflation factor bigger than twice the one he would actually need to meet the integrity risk requirements. In particular in 35% of the cases the minimum error can be smaller than half the maximum and in 60% of the cases smaller than 1.5 the maximum. These factors are proportionally degrading the protection level. Sending the integrity information in the satellite domain, allows to remove the conservatism of the worst user location concept and improve continuity and availability performance.

B. Quantile method with respect to sample standard deviation method

This section shows the performance of the quantile method described in the second section with respect to the sample standard deviation method.

Figure 15 shows, for a specific value of $\overline{G} = 10^{-4}$, α and β risk, the quantile method accuracy, i.e.

$$\frac{G_{MD} - G}{G}$$

Increasing the sample size N with respect to tail percentile G, the method accuracy increase and the minimum detectable tail gets closer to the nominal one, as it is shown in Figure 16.

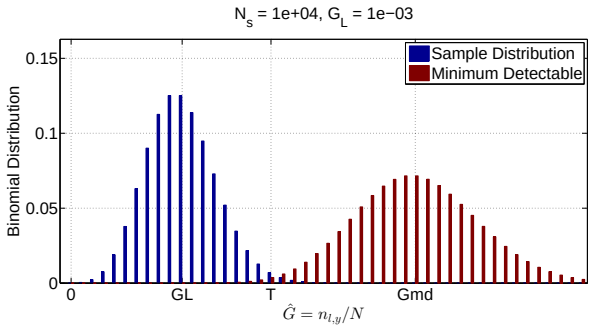

Figure 15: Estimation accuracy of the quantile method based on hypothesis testing. In this case $G = 10^-4$ and $N = 10^4$

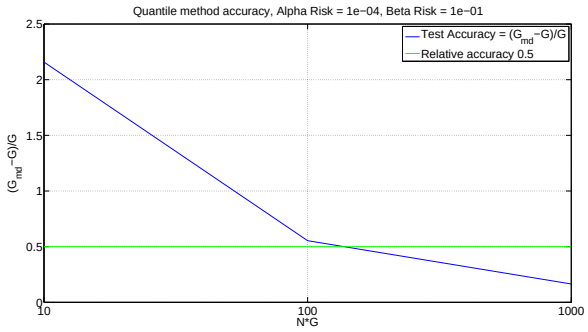

Figure 16: Quantile method estimation accuracy versus NG

In particular it is shown that to have a relative accuracy of 0.5 at least $\frac{100}{G}$ samples are required. This represents a general rule of thumb for the minimum number of samples needed to have acceptable long term monitoring accuracy. Usually it is commonly assumed that the minimum sample size needed to estimate a tail area G is $N = \frac{1}{G}$. But actually a factor 100 is needed ($N = \frac{100}{G}$) to have a sufficient estimation accuracy, as shown in Figure 16.

Figure 17 and Figure 18 shows that the quantile method provides a smaller inflation factor overall (except for percentiles smaller than 0.5 which are not relevant for integrity purpose). For $y = 2$ the inflation factor of the sample standard deviation method is even twice that of the quantile method.

C. Upper bound instead of mean value for the short term monitoring

This section describes the comparison between the vertical protection levels computed with the MHSS approach proposed in [4] with that proposed in this paper with a short latency ISM.[7].

The following parameters were used:

- $P_{HMI} = 2 \cdot 10^{-7}$,
- user grid masking angle 5

[7]The new user algorithm would foresee an estimation of the integrity risk instead of the protection level. In order to compare the two algorithms the protection level approach was used for the new user algorithm.

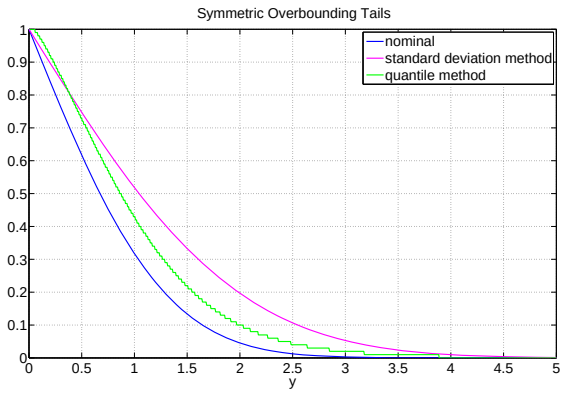

Figure 17: Comparison of sample standard deviation method versus the quantile method in terms of inflation factors of $URA(SISA)$. For the sake of simplicity for the overbounding the sum of the left and right tails are displayed in the results, although the quantile method foresees the verification separately of the left and right tails.

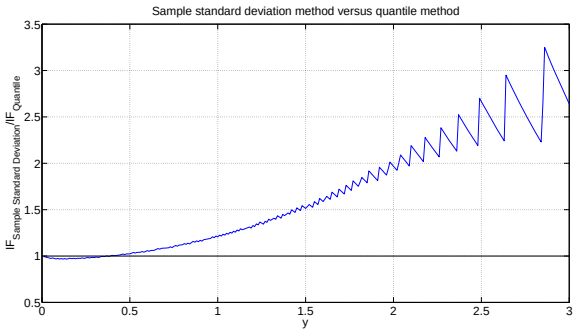

Figure 18: Ratio between the inflation factor of the sample standard deviation method and that of the quantile method

- $P_{sat} = 10^{-5}$,
- 24 GPS and 24 Galileo satellites[8],
- $\gamma = 10^{-2}$ for the short term monitoring risk ($K_{ISM} = 2.5$),
- $SISE \sim N(0.1m, 0.5m)$,
- standard deviation of the sensor station measurement noise (Gaussian distributed): $0.5m$,
- $URE = 0.5m$ for GPS and $URE = 0.67m$ for Galileo,
- $URA = 0.75m$ for GPS and $URA = 0.957m$ for Galileo,
- $B_{nom} = 0.1m$ for GPS and $B_{nom} = 0.1m$ for Galileo,
- $B_{max} = 0.75m$ for GPS and $B_{max} = 0.75m$ for Galileo.

Figure 19, Figure 20 and Figure 21 show the comparison between the protection level computed with the traditional MHSS approach and that proposed in this paper.

[8]A smaller-than-nominal constellation was chosen to allow for better visibility of the performance difference between the algorithms.

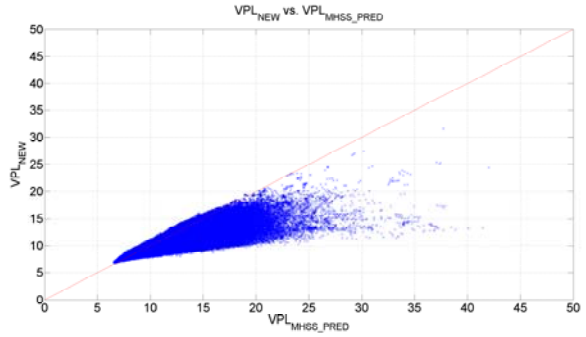

Figure 19: Comparison of MHSS versus New Protection Level

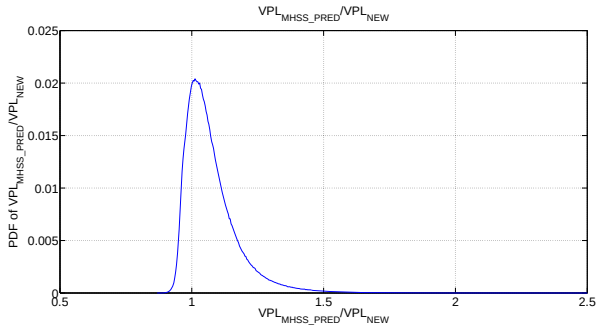

Figure 20: Probability Density Function of the ratio between the MHSS Protection Level and the New one

The user algorithm proposed by the paper improves the availability and continuity by providing smaller protection levels.

The results depends on the simulation scenario used and in particular on the risk allocated to the long and to the short term monitoring and on the ISM ground monitoring geometry. In the specific simulation scenario, 80% of the cases present a smaller protection level if computed with the new approach.

Figure 22 and Figure 23 show also the improvement of the proposed approach in terms of availability map.

D. ISM Architecture comparison

This section describes how the integrity risk is shared among the different systems involved (GNSS, ISM and user). In particular shows the impact of the proposed integrity concept and methods on the integrity risk tree. The overall tree is illustrated in Figure 24.

First of all, the result of the combination of GNSS and ISM long term monitoring on the failure occurrence probability P_{sat} is analyzed. It is observed that the ISM should perform a verification of the GNSS information with an independent methodology. It should not repeat the same satellite orbit and clock error estimation performed by the GNSS ground segment, otherwise there is no effective risk reduction. In fact the goal of the ISM monitoring is to generate a probability P_{MD} multiplying the P_{OC}. This requires an independent method, aiming to verify rather than to repeat the process.

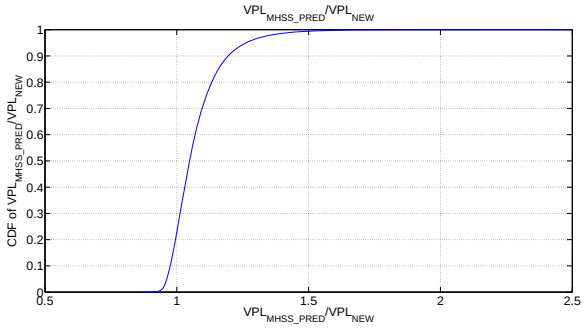

Figure 21: Cumulative Density Function of the ratio between the MHSS Protection Level and the New one

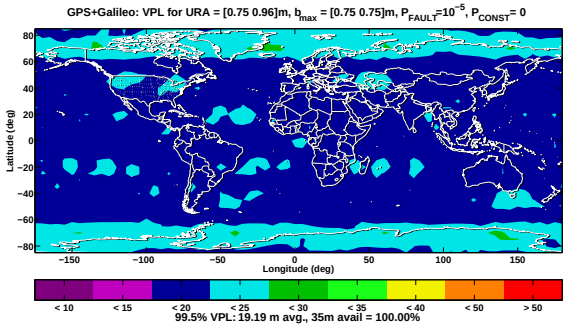

Figure 22: MHSS availability map

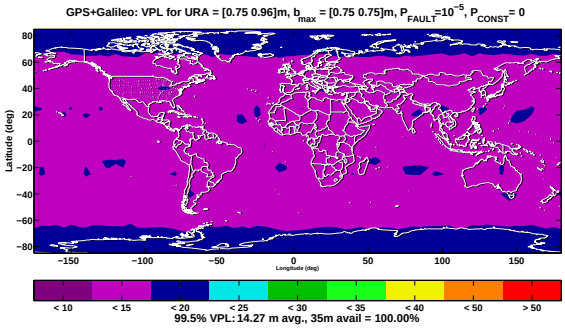

Figure 23: New approach availability map

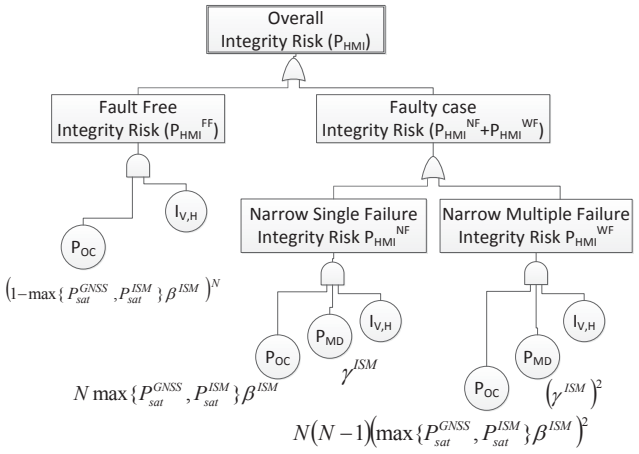

Figure 24: Integrity risk allocation tree with ISM integrity monitoring

For example the sample standard deviation method performs an overbounding estimation analogous to the GNSS ground monitoring estimation. The two corresponding risks cannot be multiplied, in fact the GNSS and the ISM observes two representations of the same stochastic process.

That is why the proposed quantile method has a different purpose: it verifies the validity of the GNSS estimation with an independent method. To perform that, it fixes a priori a false alarm probability (α-risk), and a missed detection probability (β-risk). These values are then used to compute the satellite failure probability resulting from the combination of GNSS and ISM monitoring.

For the overbounding methodology defined in the previous section, given a certain sample size N only a maximum percentile y corresponding to the tail area G can be verified. The relationship between G_{GNSS} and G_{ISM} depends on the corresponding sample size.

If $N_{ISM} \geq N_{GNSS}$, the ISM ground monitoring can verify with enough accuracy the maximum percentile y_{GNSS} referred by $URA(SISA)$. In this case the overbounding risk of the inflated URA (or SISA) is given by $G_{GNSS}\beta_{ISM}$ where β_{ISM} is the hypothesis testing β risk of the long term monitoring.

It is important for the quantile method to have enough accuracy and tune properly the different risk probabilities. In fact, as displayed in Figure 15, for all the tail areas between G and G_{MD} the missed detection probability (β risk) cannot be guaranteed. It is then important to keep this interval sufficiently small. A rigorous mathematical approach would require to consider for each tail area in between the corresponding missed detection value, defining the function of the missed detection probability versus the threat magnitude, as proposed in [14]. To keep the approach simple, it is suggested to tune the algorithm parameters and define a small interval $G_{MD} - G/G$ (e.g. 0.05). Then the corresponding β risk value can be used in the integrity tree, as shown in Figure 24.

In case instead $N_{ISM} \leq N_{GNSS}$, the maximum ISM percentile is smaller than the GNSS one: $y_{ISM} \leq y_{GNSS}$. The conclusion is that

$$G_{GNSS+ISM} \cong max(G_{GNSS}, G_{ISM})\beta_{ISM}$$

From this relationship, it can be concluded that the ISM long term monitoring leads to an appreciable integrity risk reduction if $G_{ISM} \leq G_{GNSS}$, i.e. if the ISM sample size is larger than the GNSS one. The realization of this might face feasibility problems.

The short term monitoring however has a different effect. In fact the γ risk, defined in the short term monitoring, directly multiplies the $G_{GNSS+ISM}$ risk and the risk reduction can be more effective.

In both cases it is shown how the real added value in terms of risk reduction results by ISM ground monitoring methods which verify the GNSS performance more

than repeat an analogous monitoring. This leads to risk probability reduction through probability multiplication.

IV. Conclusion

The design of an ISM architecture enabling the fulfillment of the ICAO precision approach requirements with a stand alone GNSS receiver is an interesting topic, while its details are challenging due to ambitious goals.

First of all the overbounding methodology has to meet the integrity risk requirements expressed in terms of small probabilities with a limited amount of data. Several methods have been investigated in the past, but they have strict assumptions and are extremely conservative.

This paper uses a different approach. It fixes the overbounding risk as the maximum tail area estimable with the available sample size, defining it as threat and modelling it in the satellite failure probability P_{sat}. This allows to relax the GNSS ground monitoring design requirements and consequently the number of needed sensor and uplink stations.

Besides it proposes two ISM ground monitoring algorithms: a long term monitoring covering the fault free case using a quantile method based on an hypothesis testing approach. This method improves continuity and availability through reduced ISM inflation factors with respect to usual sample standard deviation method. Secondly a short term monitoring is proposed, where the maximum Signal In Space errors rather than conservative mean values are estimated. This additional monitoring allows to relax the receiver design requirements and to have simple user algorithms. Finally a different ISM content with respect to the present definition is proposed. The combination of these proposals improve the continuity and availability performances providing reduced protection levels.

The overall study provides guidelines and recommendations for an optimum ISM architecture design, in order to have an efficient and effective integrity risk reduction both for the GNSS ground segment and for the user. The best ISM performance can be reached if the ISM long term monitoring system uses a longer observation interval than the GNSS ground segment. This might be unfeasible due to the lack of historic data. On the other side the short term monitoring can also provide an effective and significant risk reduction. The paper provides methodologies to quantify the ISM monitoring performance and compute the architecture design parameters.

A potential improvement of the system performance with respect to present algorithms is demonstrated by means of Monte Carlo simulations. The validation of this activity with real data is ongoing. In particular a global monitoring network of around 15 stations, available at DLR (EVnet and Congo), will be used to characterize GNSS constellation threats, estimate ISM and investigate ARAIM algorithms. The user ARAIM algorithm performance will be then finally verified during a flight campaign.

References

[1] ICAO, Annex 10, Aeronautical Telecommunications, Volume 1, Amendment 84, published 20 July 2009. GNSS standards and recommended practices (SARPs) in Section 3.7 and subsections, Appendix B, and Attachment D.

[2] Phase II of the GNSS Evolutionary Architecture Study, February 2010. ⟨http://www.faa.gov/about/office_org/headquarters_offices/ato/service_units/techops/navservices/gnss/library/documents/media/GEASPhaseII_Final.pdf⟩

[3] RTCA DO-246D, December 16, 2008, "GNSS-Based Precision Approach Local Area Augmentation System (LAAS) Signal-In-Space Interface Control Document (ICD)", Section 2.1. "RF Transmission Characteristics"

[4] GPS-Galileo Working Group C ARAIM Technical Subgroup Interim Report (Issue 1.0, 19 December 2012) http://www.gps.gov/policy/cooperation/europe/2013/working-group-c/ARAIM-report-1.0.pdf

[5] J. Mach et al. 'Making GNSS Integrity Simple and Efficient A New Concept Based on Signal-in-Space Error Bounds', in Proceedings of the ION GNSS 2006, Forth Worth, TX

[6] DeCleene B (2000) 'Defining Pseudorange Integrity Overbounding', in Proceedings of the ION GPS 2000, 1916-1924.

[7] Oehler V et al., 'The Galileo Integrity Concept', in Proceedings of the ION GNSS 2004, Long Beach CA

[8] Carlos Hernandez Medel et al., 'The Galileo Ground Segment Integrity Algorithms: Design and Performance', International Journal of Navigation and Observation, Volume 2008, Article ID 178927

[9] Schempp, T. R. and Rubin, A. L., 'An Application of Gaussian Bounding for the WAAS Fault-Free Error Analysis', in Proceedings of the ION GPS meeting, Portland, OR, 2002.

[10] Rife J, Pullen S, Pervan B, and Enge P., 'Paired overbounding and application to GPS augmentation', in Proceedings IEEE Position, Location and Navigation Symposium, Monterey, California, April 2004.

[11] Rife J, Pullen S, Pervan B, and Enge P., 'Core overbounding and its implications for LAAS integrity', in Proceedings of ION GNSS 2004, Long Beach, California, September, 2004.

[12] Rife J, Walter T, and Blanch J, 'Overbounding SBAS and GBAS error distributions with excess-mass functions', in Proceedings of the 2004 International Symposium on GPS/GNSS, Sydney, Australia, 6-8 December, 2004.

[13] Blanch at al., 'An Optimized Multiple Solution Separation RAIM Algorithm for Vertical Guidance', in Proceedings of the ION GNSS 2007, Forth Worth, TX, September 2007

[14] F. Amarillo, P. D'Angelo, 'New Developments for the user Integrity Processing with Galileo Implementation and Testing of Galileo user Integrity Algorithms', in Proceedings of the 22nd International Meetingof the Satellite Division of The Institute of Navigation, Savannah, GA, Semptember 2009

[15] Blanch at al., 'Understanding PHMI for Safety of life application in GNSS', in Proceedings of the ION NTM 2007, San Diego, California, January 2007